Supporting Information

High piezoelectric, dielectric relaxation and semiconductor properties in an one-dimension organic-inorganic hybrid complexes: [2-methyl-1,5-pentanediamine][$BiCl_5$]†

Zheng-Hui Hu, Xin-Yu Liu, Shu-Qi Sun, Chen Gong, Nuo Liu, Ji-Xing Gao*

Anhui Provincical Key Laboratory for Degradation and Monitoring of Pollution of the Environment, School of Chemistry and Materials Engineering, Fuyang Normal University, Fuyang 236037, P. R. China.

E-mail: gaojx@fynu.edu.cn.

Experimental section

Synthesis.

[2-MPDA][BiX_5] (2-MPDA =2-methyl-1,5-pentanediamine, X = Cl, Br, I) was prepared through the reaction of Bi_2O_3 (99.0 %) and 2-methyl-1,5-pentanediamine (98 %) in a solution of HCl (36 %), HBr (40 %), HI (45.0 ~ 50.0 %, ≤ 1.5 % H_3PO_2), respectively. Firstly, moderate HX was added dropwise into Bi_2O_3 (0.233 g, 0.5 mmol) under stirring to obtain clear SbI_3 solution. Afterwards, 2-methyl-1,5-pentanediamine (0.117 g, 1 mmol) was added into the SbX_3 solution under heating and stirring towards complete dissolution. Colourless/Yellow/Red crystals were grown by heating evaporation on a constant temperature heating table after one day. Polycrystalline samples were prepared through grinding the dried crystals into fine powder. IR (Infrared Spectra) and PXRD (Powder X-Ray Diffraction) measurements were performed to verify the purity of [2-MPDA][BiX_5], as shown in Fig. S1 and Fig. S2).

Single-Crystal X-ray Crystallography.

Variable-temperature X-ray single-crystal diffraction data at 93, 223, and 293 K were collected on a *Rigaku Varimax™ DW* diffractometer with *Mo–Kα* radiation (λ = 0.71073 Å) by using four-circle measurement method. The *Hypix-6000HE* detector and Crystalclear software package (*Rigaku OD*, 2018) was used for collection of diffraction data and data processing including empirical absorption corrections, respectively. The structures were solved by direct methods and refined by the fullmatrix method based on F^2 using the SHELXLTL software package. All nonhydrogen atoms were refined anisotropically using all reflections with $I > 2\sigma(I)$. The positions of the hydrogen atoms were generated geometrically and refined using a "riding" model with Uiso = 1.2Ueq (C and N). The molecular structures and the packing views were drawn with *DIAMOND* (Brandenburg and Putz, 2005). Angles and distances between some atoms were carried out using *DIAMOND*, and other calculations were calculated using *SHELXLTL*. Each temperature point, using Oxford Cryostream CS800 variable temperature system, the sample is protected by two layers of gas, the outer layer is compressed dry air, the inner layer is heated to the specified temperature of liquid

nitrogen. Crystallographic data and structure refinement at 93, 223, and 293 K of [2-MPDA][$BiCl_5$] are list in Table S1, and at 93 and 293 K of [2-MPDA][$BiBr_5$] and [2-MPDA][BiI_5] are list in Table S2 and Table S3, respectively.

TGA and DSC Measurements.

Polycrystalline sample (9.15 mg) of **1** were used for the TGA measurements over the temperature range 300 K to 1000 K on a Perkin-Elmer Diamond TGA instrument with rate of 10 K min^{-1} under the protection of nitrogen at atmospheric pressure in aluminum crucibles to verify its thermal stability. Polycrystalline sample (30.0 mg) of **1** were used for the DSC measurements over the temperature range 140 K to 220 K on a QSC 214 polyma instrument with rate of 10 K min^{-1} under the protection of nitrogen at atmospheric pressure in aluminum crucibles.

Dielectric measurements.

The pressed-powder pellet of **1**, **2** and **3** (with an area of 8.6, 9.5 and 8.6 mm^2 and a thickness of 0.39, 0.45 and 0.29 mm, respectively) were sandwiched by carbon conducting glue between two parallel copper electrodes for dielectric constant measurements. Dielectric permittivity ε ($\varepsilon = \varepsilon' - i\varepsilon''$) of **1** was measured on a Tonghui TH2828A analyzer over the frequency range of 500 Hz to 1 MHz and in the temperature range 90 K to 300 K with rate of 10 K min^{-1}. The applied voltage in the measurements was 1 V.

Cole-Cole relation.

$$\varepsilon = \varepsilon_\infty + \frac{\varepsilon_0 - \varepsilon_\infty}{1 + (i\omega\tau)^{1-\alpha}} \quad (1)$$

Where ε_0 and ε_∞ are respectively the low and high frequency limits of the dielectric permittivity, ω is angular frequency, τ is the macroscopic dielectric relaxation time and α is a parameter characterizing the distribution of the relaxation times.

SHG measurements. Variable-temperature second harmonic generation (SHG) experiments were executed by Kurtz-Perry powder SHG test using an unexpanded laser beam with low divergence (pulsed Nd:YAG at a wavelength of 1064 nm, 5 ns pulse duration, 1.6 MW peak power, 10 Hz repetition rate). The instrument model is Ins 1210058, INSTEC Instruments, while the laser is Vibrant 355 II, OPOTEK. The numerical values of the nonlinear optical coefficients for SHG have been determined by comparison with a KDP (KH_2PO_4, potassium dihydrogen phosphate) reference.

Piezoelectric coefficient measurements. The macroscopic piezoelectric coefficient (d_{33}) was measured by a commercial piezometer (Piezotest, model:

PM200) using "Berlincourt" method (also called "quasi-static" method). The sample crystal (5.1×1.3×1.1 mm) was placed in between two flat metal plates which clamp the sample and apply a small oscillating force (5 N) along the normal direction, while the piezoelectric charge is measured. The Berlincourt method is a simple and straightforward way to measure the direct piezoelectric coefficient, d_{33}. All measured crystals were selected with defined shape and the aspect ratio is more than 3 to ensure the d_{33} is correctly measured. The maximum of d_{33} value was found along the polar-axis of the sample crystal, which is near the proximity of <001> direction.

A.c. conductivity.

The a.c. conductivity $\sigma_{a.c.}$ of single-crystal **1** and **2** along the c axis at frequency 500 Hz was obtained from the imaginary part of the dielectric permittivity ε" by using the relation: $\sigma_{a.c.} = \omega\varepsilon''\varepsilon_0$, where ω is the angular frequency $2\pi f$ and ε_0 is the permittivity of free space (8.854×10^{-12} F m^{-1}).

UV-vis diffuse-reflectance spectra measurements.

UV-vis diffuse-reflectance spectra measurements were performed at room temperature using a Shimadzu UV-2450 spectrophotometer mounted with ISR-2200 integrating sphere operating from 200 to 1100 nm. $BaSO_4$ was used as a 100 % reflectance reference. Powdered crystal of HDA-BiI_5 was prepared for measurement. The generated reflectance-versus-wavelength data were used to estimate the band gap of **1**, **2** and **3** the material by converting reflectance data to absorbance according to the Kubelka−Munk equation: $F(R_\infty) = (1 - R_\infty)^2/2R_\infty$. The optical band gap can be determined by the variant of the Tauc equation: $(h\nu \cdot F(R_\infty))^{1/n} = A(h\nu - E_g)$, Where: h: Planck's constant, ν: frequency of vibration, $F(R_\infty)$: Kubelka−Munk equation, E_g: band gap, A: proportional constant. The value of the exponent n denotes the nature of the sample transition. For direct allowed transition, n = 1/2; for indirect allowed transition, n = 2. Hence, the optical band gap E_g can be obtained from a Tauc plot by plotting $(h\nu \cdot F(R_\infty))^{1/n}$ against the energy in eV and extrapolation of the linear region to the X-axis intercept.

Calculation of energy band structure and density of states for Compound 1.

The band gaps and PDOS (density of states) of compound **1** were calculated by using the CASTEP module of Accelrys Materials Studio 8.0. First, the structure file of compound 1 in". CIF" format was converted into".mol" format by software such as Mercury 3.3 or diamond 3.2. Then, after importing into Accelrys Materials Studio 8.0, we set up the structure optimization and calculate

the relevant parameters, carry on the structure optimization and the calculation of each item (band structure and density of states). Among them, quality: “fine”, max. iterations: “100”, tick before the “optimize cell”, functional: “GGA” and “PBE”, use "TS" method for DFT-D correction (considering the interaction between molecules), energy tolerances per: “Atom”, pseudopotentials: “on the fly”, set the band structure scan path in the Brillouin zone and so on. Finally, the data were exported, and the OriginLab Origin V8.0 was used to do the graph and result analysis.

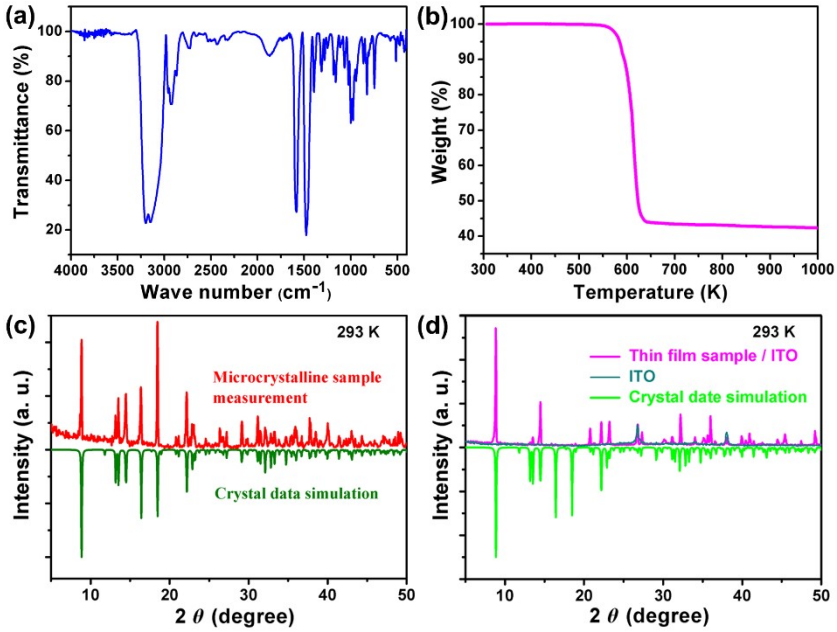

Fig. S1 (a) IR spectrum of **1** at room temperature. (b) TGA curve of **1**. PXRD of microcrystalline sample (c) and thin film sample (d) of 1 at room temperature.

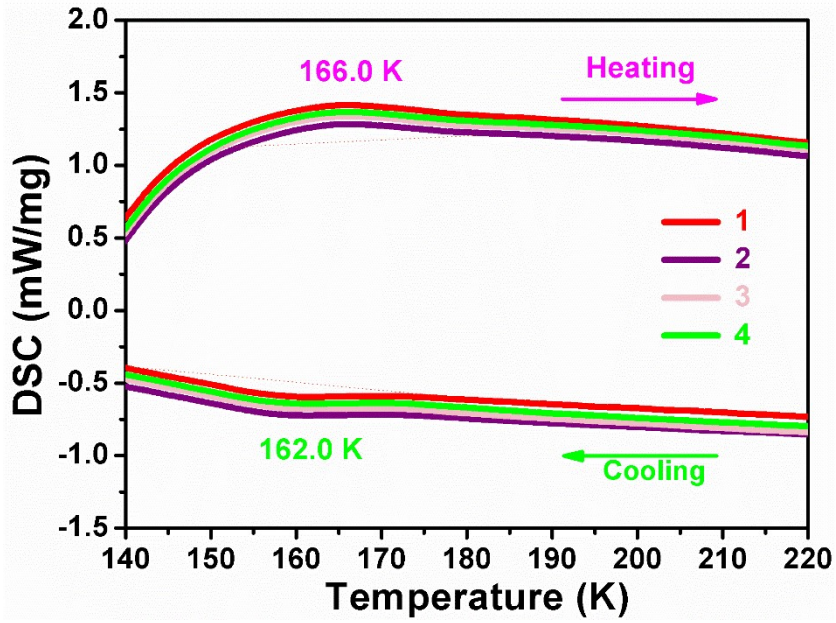

Fig. S2 DSC curve cycles of **1**.

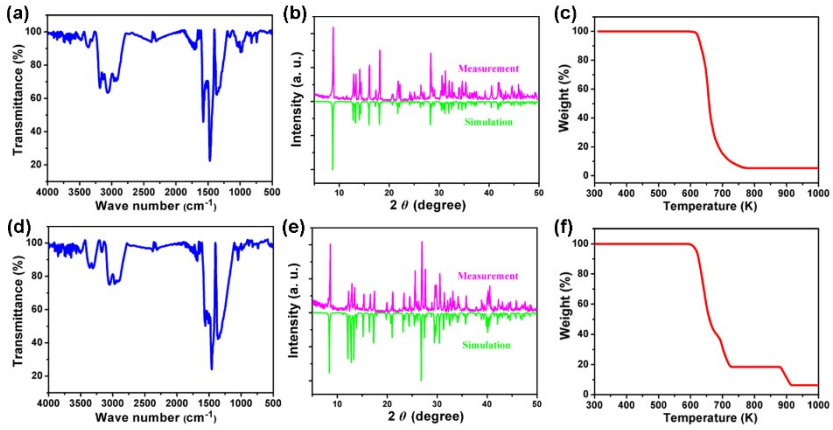

Fig. S3 (a), (b), (c) and (d), (e), (f) are IR spectrum, PXRD, TGA of microcrystalline sample of **2** and **3**, respectively.

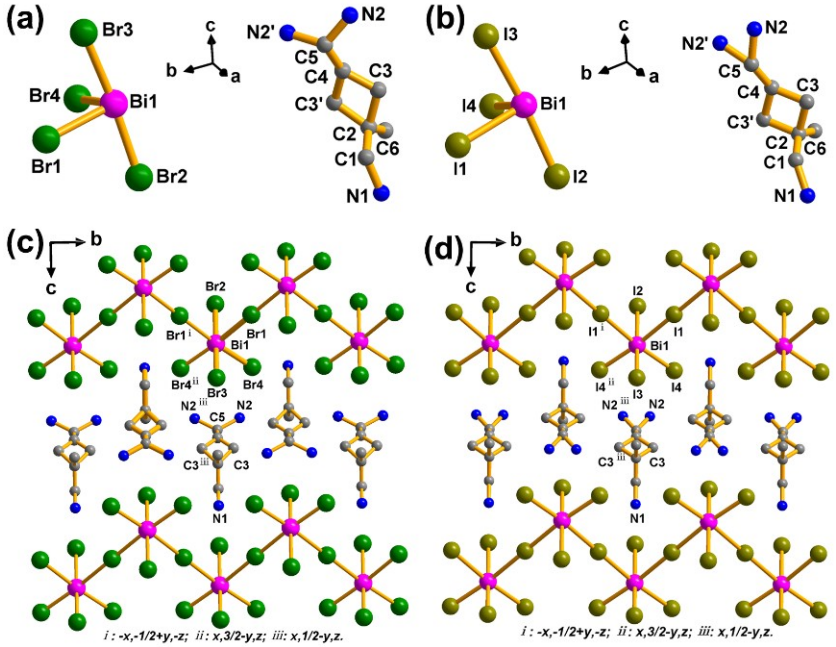

Fig. S4 Minimum asymmetric unit and packing structures of **2** (a, c) and **3** (b, d) at 93 K. Hydrogen atoms are omitted for clarity.

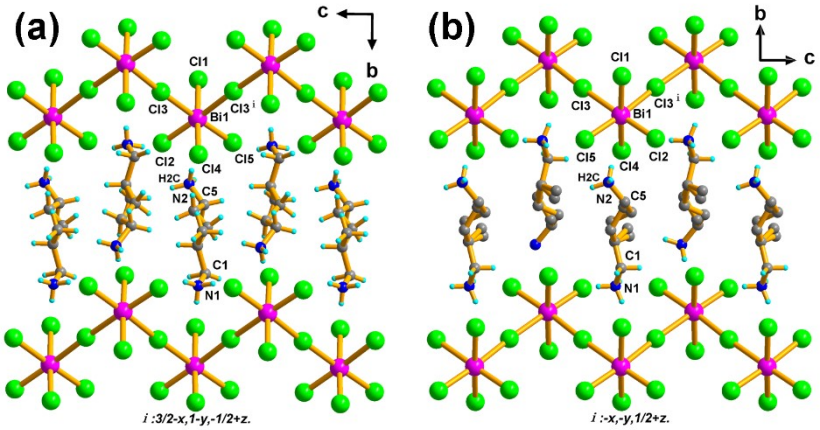

Fig. S5 Packing structures of **1** at 93 K (a) and 293 K (b) along a-axis. For structures at 293 K, disordered hydrogen atoms are omitted for clarity.

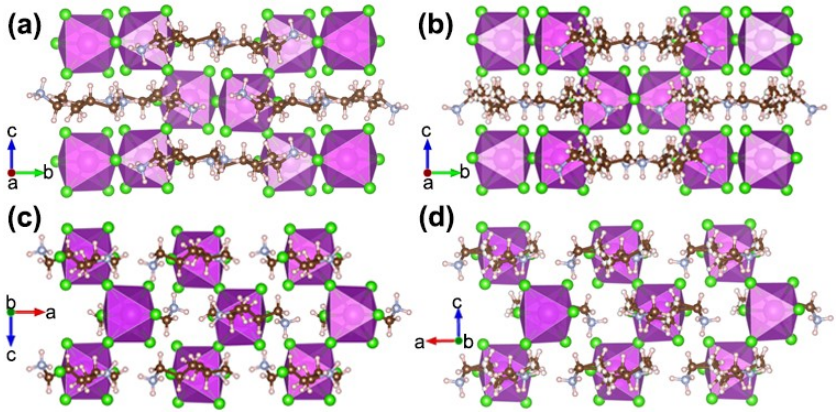

Fig. S6 Packing structures of **1** at 93 K ((a) and (c)) and 293 K ((b) and (d)) in the polyhedron style along a-axis and b-axis.

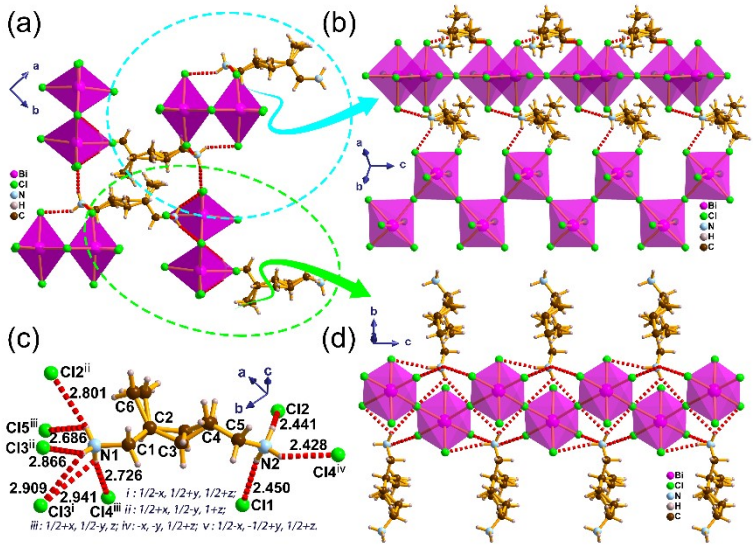

Fig. S7 Hydrogen bonds (a, b, d) of **1** and hydrogen bonds environment of cation (c) of **1** at 293 K.

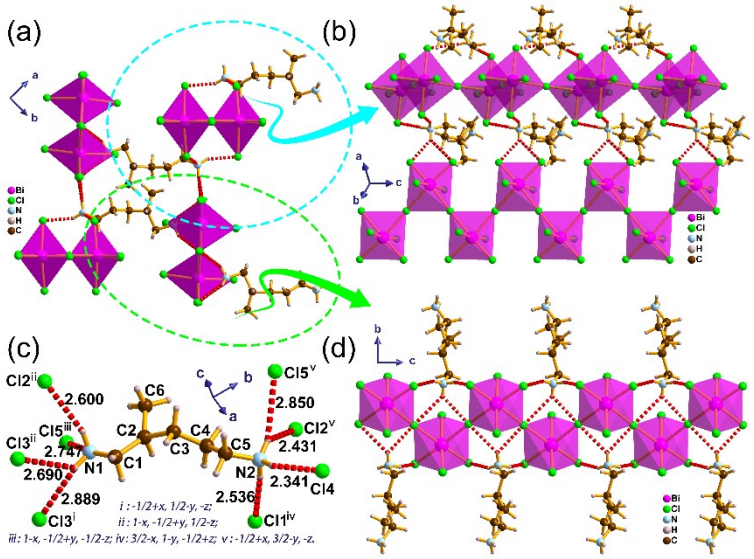

Fig. S8 Hydrogen bonds (a, b, d) of **1** and hydrogen bonds environment of cation (c) of **1** at 93 K.

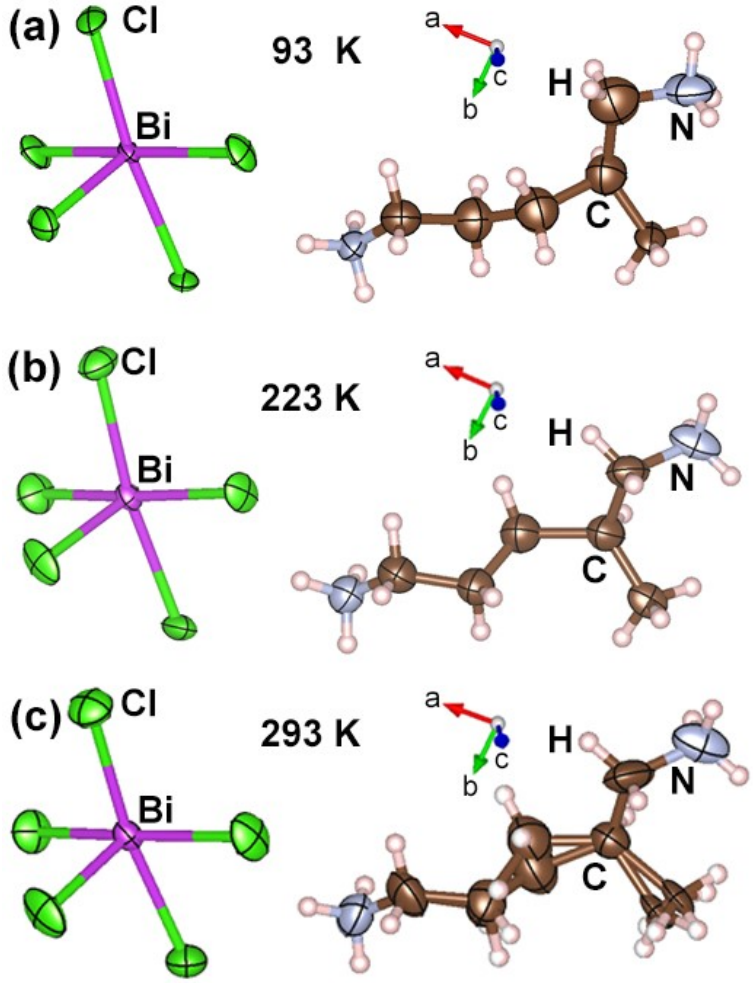

Fig. S9 View of the asymmetric units of **1** obtained at 93 K, 223 K and 293 K showing the atomic numbering scheme. Displacement ellipsoids are drawn at the 30% probability level. C and Cl atoms of cations are labeled to see more clearly.

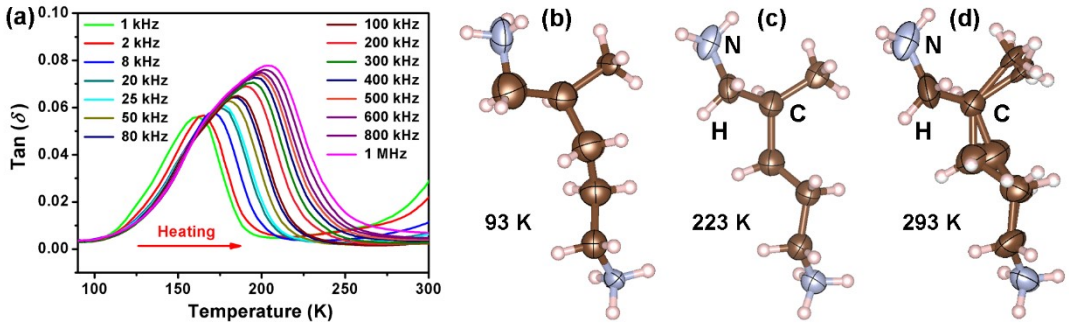

Fig. S10 Temperature-dependence of the dielectric loss (tan(δ)) (b) of the polycrystalline sample of **1** at different frequency.

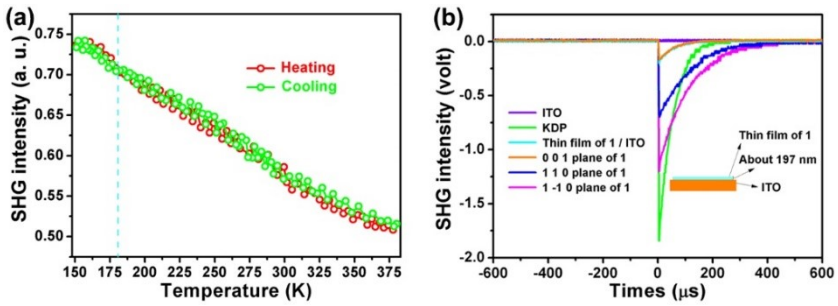

Fig. S11 VT-SHG (Variable temperature second-order nonlinear) of **1** (a). SHG intensity of **1** (b) at 293 K. SHG intensity of KDP and **1** in different states.

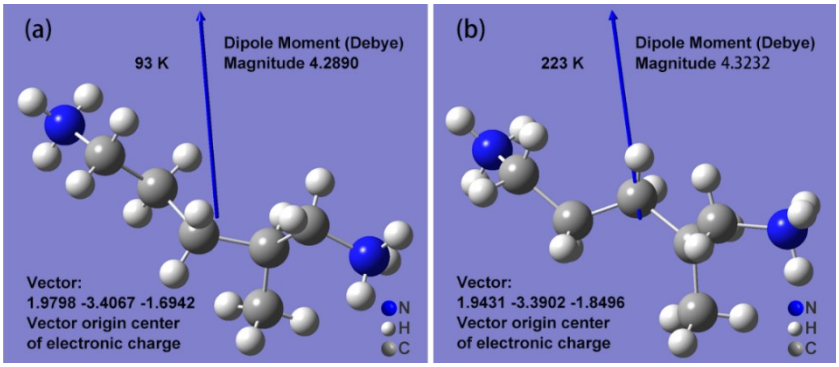

Fig. S12 Dipole moment direction and magnitude the cation of **1** at 93 K and 223 K were calculated through GaussView 5.0.9 software.

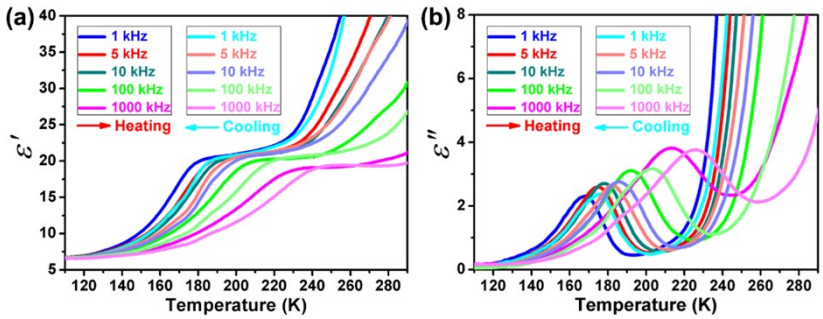

Fig. S13 Temperature dependence of the real part ε' (a) and imaginary part ε'' (b) of the dielectric constant of **2** measured results at selected frequencies between 1 kHz and 1000 kHz in a heating and cooling process.

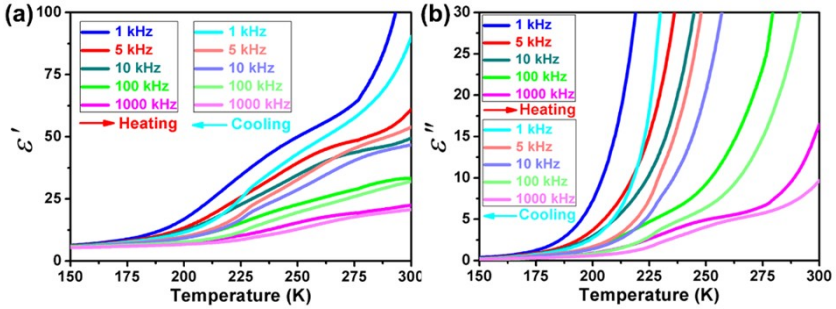

Fig. S14 Temperature dependence of the real part ε' (a) and imaginary part ε'' (b) of the dielectric constant of **3** measured results at selected frequencies between 1 kHz and 1000 kHz in heating and cooling process.

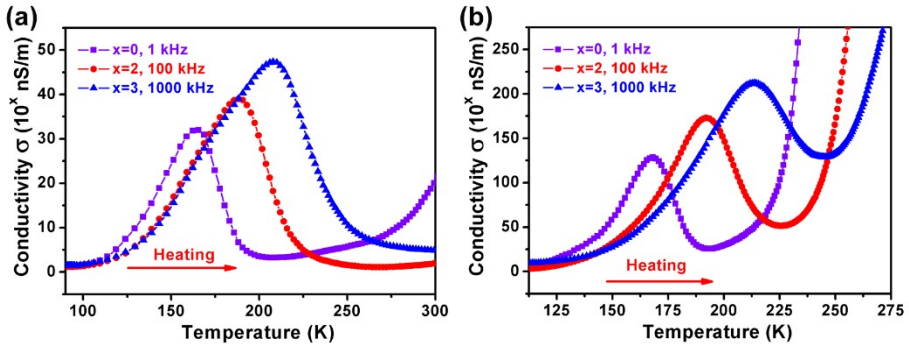

Fig. S15 T-$\sigma_{a.c.}$ curves of **1** (a) and **2** (b) at frequency 1, 100 and 1000 kHz in heating process.

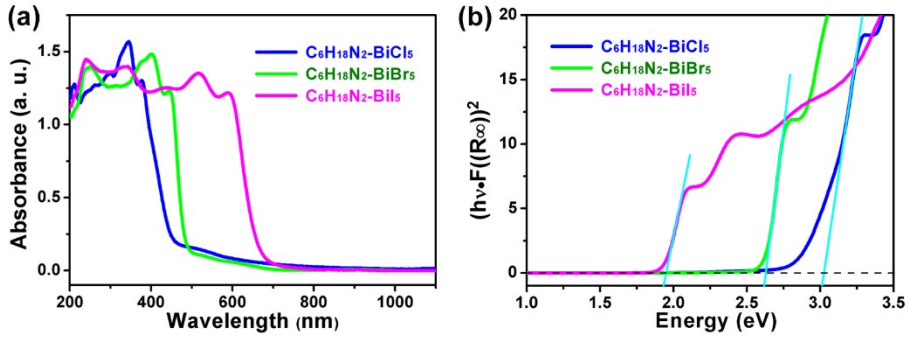

Fig. S16 (a) Ultraviolet-vis absorption spectrum of **1**, **2** and **3** (a). The tauc plot and the E_g is about 3.0, 2.6 and 1.9 eV of **1**, **2** and **3** (b).

Table S1 Crystal data and structure refinement for **1** at 93, 223 and 293 K.

	93 K	223 K	293 K
Empirical formula	$C_6H_{18}N_2BiCl_5$	$C_6H_{18}N_2BiCl_5$	$C_6H_{18}N_2BiCl_5$
Formula weight	504.45	504.45	504.45
Crystal system	Orthorhombic	Orthorhombic	Orthorhombic
Space group	$P2_12_12_1$	$Pna2_1$	$Pna2_1$
a (Å)	14.9168(9)	14.9838(5)	14.9944(5)
b (Å)	13.1553(7)	13.2925(4)	13.3505(4)
c (Å)	7.6806(5)	7.7386(2)	7.7677(2)
Volume (Å^3)	1507.20(16)	1541.31(8)	1554.96(8)
Z, D_{calcd} / g cm^{-3}	4, 2.223	4, 2.174	4, 2.155
μ (mm^{-1})	12.556	12.278	12.170
F(000)	944	944	944
Goodness-of-fit on F^2	1.000	1.025	1.045
Theta range (deg.)	2.731 ~ 25.023	2.719 ~ 26.995	2.717 ~ 26.994
Completeness to theta	99.8	99.9	99.9
R(int)	0.0576	0.0381	0.0378
R_1 [a] (> 2σ)	0.0853	0.0411	0.0350
wR_2 [b] (> 2σ)	0.1978	0.0909	0.0834

[a] $R_1 = \Sigma||F_o| - |F_c||/\Sigma|F_o|$, [b] $wR_2 = [\Sigma(|F_o|^2 - |F_c|^2) / \Sigma|F_o|^2]^{1/2}$

Table S2 Crystal data and structure refinement for **2** at 93 and 293 K.

	93 K	**293 K**
Empirical formula	$C_6H_{18}N_2BiBr_5$	$C_6H_{18}N_2BiBr_5$
Formula weight	726.70	726.70
Crystal system	Orthorhombic	Orthorhombic
Space group	*Pnma*	*Pnma*
a (Å)	15.2463(11)	15.3618(6)
b (Å)	7.9575(6)	8.0509(3)
c (Å)	13.4076(8)	13.5870(4)
Volume (Å^3)	1626.6(2)	1680.39(10)
Z, D_{calcd} / g cm^{-3}	4, 2.968	4, 2.873
μ (mm^{-1})	23.095	22.357
F(000)	1304	1304
Goodness-of-fit on F^2	1.010	1.001
Theta range (deg.)	2.672 ~ 25.230	2.652 ~ 27.243
Completeness to theta	99.5	99.9
R(int)	0.3666	0.1235
R_1 [a] (> 2σ)	0.2489	0.0554
wR_2 [b] (> 2σ)	0.6235	0.1309

[a] $R_1 = \Sigma||F_o| - |F_c||/\Sigma|F_o|$, [b] $wR_2 = [\Sigma(|F_o|^2 - |F_c|^2) / \Sigma|F_o|^2]^{1/2}$

Table S3 Crystal data and structure refinement for **3** at 93 and 293 K.

	93 K	**293 K**
Empirical formula	$C_6H_{18}N_2BiI_5$	$C_6H_{18}N_2BiI_5$
Formula weight	961.70	961.70
Crystal system	Orthorhombic	Orthorhombic
Space group	*Pnma*	*Pnma*
a (Å)	15.8297(6)	15.9510(8)
b (Å)	8.5091(3)	8.5792(4)
c (Å)	13.7812(5)	13.9712(6)
Volume (Å^3)	1856.28(12)	1911.91(15)
Z, D_{calcd} / g cm^{-3}	4, 3.441	4, 3.341
μ (mm^{-1})	17.792	17.275
F(000)	1664	1664
Goodness-of-fit on F^2	1.023	1.252
Theta range (deg.)	2.573 ~ 25.247	2.554 ~ 25.248
Completeness to theta	99.4	99.5
R(int)	0.1883	0.2395
R_1 [a] (> 2σ)	0.1591	0.1240
wR_2 [b] (> 2σ)	0.5483	0.3227

[a] $R_1 = \Sigma||F_o| - |F_c||/\Sigma|F_o|$, [b] $wR_2 = [\Sigma(|F_o|^2 - |F_c|^2) / \Sigma|F_o|^2]^{1/2}$

Table S4 Bond lengths [A] and angles [deg] for **1** at 93, 223 and 293 K.

93 K			
Bi(1)-Cl(2)	2.569(5)	N(1)-C(1)	1.442(12)
Bi(1)-Cl(5)	2.591(5)	N(2)-C(5)	1.441(13)
Bi(1)-Cl(1)	2.641(3)	C(1)-C(2)	1.634(8)
Bi(1)-Cl(4)	2.722(3)	C(2)-C(6)	1.430(9)
Bi(1)-Cl(3)#1	2.836(6)	C(2)-C(3)	1.472(9)
Bi(1)-Cl(3)	2.872(6)	C(3)-C(4)	1.431(12)
Cl(3)-Bi(1)#2	2.836(6)	C(4)-C(5)	1.458(12)
Cl(2)-Bi(1)-Cl(5)	93.01(16)	Cl(1)-Bi(1)-Cl(3)#1	85.97(19)
Cl(2)-Bi(1)-Cl(1)	96.75(17)	Cl(4)-Bi(1)-Cl(3)#1	87.98(18)
Cl(5)-Bi(1)-Cl(1)	93.60(17)	Cl(2)-Bi(1)-Cl(3)	90.40(17)
Cl(2)-Bi(1)-Cl(4)	89.02(15)	Cl(5)-Bi(1)-Cl(3)	175.85(18)
Cl(5)-Bi(1)-Cl(4)	89.58(15)	Cl(1)-Bi(1)-Cl(3)	88.33(19)
Cl(1)-Bi(1)-Cl(4)	173.25(11)	Cl(4)-Bi(1)-Cl(3)	88.12(18)
Cl(2)-Bi(1)-Cl(3)#1	174.24(18)	Cl(3)#1-Bi(1)-Cl(3)	84.588(12)
Cl(5)-Bi(1)-Cl(3)#1	91.88(17)	Bi(1)#2-Cl(3)-Bi(1)	177.7(3)
N(1)-C(1)-C(2)	94.2(7)	C(4)-C(3)-C(2)	128.9(9)
C(6)-C(2)-C(3)	98.8(6)	C(3)-C(4)-C(5)	119.8(10)
C(6)-C(2)-C(1)	133.3(8)	N(2)-C(5)-C(4)	104.9(9)
C(3)-C(2)-C(1)	108.0(6)		
223 K			
Bi(1)-Cl(5)	2.548(4)	N(1)-C(1)	1.434(16)
Bi(1)-Cl(2)	2.599(5)	N(2)-C(5)	1.422(16)
Bi(1)-Cl(1)	2.650(3)	C(1)-C(2)	1.468(15)
Bi(1)-Cl(4)	2.722(3)	C(2)-C(6)	1.452(15)
Bi(1)-Cl(3)#1	2.761(5)	C(2)-C(3)	1.576(14)
Bi(1)-Cl(3)	2.983(5)	C(3)-C(4)	1.388(16)
Cl(3)-Bi(1)#2	2.761(5)	C(4)-C(5)	1.452(15)
Cl(5)-Bi(1)-Cl(2)	93.99(12)	Cl(1)-Bi(1)-Cl(3)#1	84.89(17)
Cl(5)-Bi(1)-Cl(1)	95.48(18)	Cl(4)-Bi(1)-Cl(3)#1	89.79(17)
Cl(2)-Bi(1)-Cl(1)	95.26(18)	Cl(5)-Bi(1)-Cl(3)	175.63(15)
Cl(5)-Bi(1)-Cl(4)	90.24(16)	Cl(2)-Bi(1)-Cl(3)	87.59(16)
Cl(2)-Bi(1)-Cl(4)	89.31(18)	Cl(1)-Bi(1)-Cl(3)	88.43(18)
Cl(1)-Bi(1)-Cl(4)	172.40(10)	Cl(4)-Bi(1)-Cl(3)	85.69(16)
Cl(5)-Bi(1)-Cl(3)#1	93.43(16)	Cl(3)#1-Bi(1)-Cl(3)	84.943(18)
Cl(2)-Bi(1)-Cl(3)#1	172.52(17)	Bi(1)#2-Cl(3)-Bi(1)	173.6(2)
N(1)-C(1)-C(2)	108.9(13)	C(4)-C(3)-C(2)	121.2(13)
C(6)-C(2)-C(1)	119.7(13)	C(3)-C(4)-C(5)	120.0(13)
C(6)-C(2)-C(3)	121.3(10)	N(2)-C(5)-C(4)	124.0(14)
C(1)-C(2)-C(3)	112.1(11)		

293 K			
Bi(1)-Cl(2)	2.560(7)	Bi(1)-Cl(3)#1	2.830(11)
Bi(1)-Cl(5)	2.567(8)	Bi(1)-Cl(3)	2.917(10)
Bi(1)-Cl(1)	2.654(3)	Cl(3)-Bi(1)#2	2.830(11)
Bi(1)-Cl(4)	2.721(3)		
Cl(2)-Bi(1)-Cl(5)	94.42(14)	Cl(1)-Bi(1)-Cl(3)#1	85.3(4)
Cl(2)-Bi(1)-Cl(1)	97.9(3)	Cl(4)-Bi(1)-Cl(3)#1	87.3(4)
Cl(5)-Bi(1)-Cl(1)	92.8(3)	Cl(2)-Bi(1)-Cl(3)	87.5(3)
Cl(2)-Bi(1)-Cl(4)	88.9(3)	Cl(5)-Bi(1)-Cl(3)	178.0(3)
Cl(5)-Bi(1)-Cl(4)	91.2(3)	Cl(1)-Bi(1)-Cl(3)	87.6(4)
Cl(1)-Bi(1)-Cl(4)	171.74(15)	Cl(4)-Bi(1)-Cl(3)	88.2(4)
Cl(2)-Bi(1)-Cl(3)#1	171.7(3)	Cl(3)#1-Bi(1)-Cl(3)	85.029(15)
Cl(5)-Bi(1)-Cl(3)#1	93.0(4)	Bi(1)#2-Cl(3)-Bi(1)	176.8(6)

Symmetry transformations used to generate equivalent atoms : 93 K, #1 -x+3/2,-y+1,z-1/2; #2 -x+3/2,-y+1,z+1/2. 223 K, #1 -x,-y,z+1/2; #2 -x,-y,z-1/2. 293 K, #1 -x,-y,z+1/2; #2 -x,-y,z-1/2.

Table S5 Hydrogen bonds parameters for **1** at 93, 223 and 223 K.

D-H···A	D-H	H···A	D···A	∠D-H···A
93 K				
N(1)-H(1A)...Cl(3)#3	0.90	2.69	3.310(16)	127.1
N(1)-H(1A)...Cl(3)#4	0.90	2.89	3.563(16)	133.2
N(1)-H(1B)...Cl(5)#5	0.90	2.74	3.566(15)	152.4
N(1)-H(1C)...Cl(2)#3	0.90	2.60	3.345(15)	141.2
N(2)-H(2A)...Cl(4)	0.90	2.34	3.176(10)	154.0
N(2)-H(2B)...Cl(2)#6	0.90	2.43	3.099(11)	131.2
N(2)-H(2B)...Cl(5)#6	0.90	2.85	3.577(11)	138.8
N(2)-H(2C)...Cl(1)#1	0.90	2.54	3.432(14)	172.9
C(5)-H(5B)...Cl(1)#2	0.96	2.70	3.620(14)	161.8
223 K				
N(1)-H(1A)...Cl(3)#4	0.90	2.72	3.498(13)	145.4
N(1)-H(1A)...Cl(3)#7	0.90	2.84	3.379(13)	119.6
N(1)-H(1B)...Cl(2)#4	0.90	2.75	3.555(15)	149.0
N(1)-H(1B)...Cl(5)#6	0.90	2.93	3.358(15)	111.1
N(1)-H(1C)...Cl(4)#6	0.90	2.62	3.516(15)	171.6
N(2)-H(2A)...Cl(4)#1	0.90	2.42	3.186(13)	142.5
N(2)-H(2B)...Cl(1)	0.90	2.62	3.496(15)	164.7
N(2)-H(2C)...Cl(2)#5	0.90	2.54	3.140(14)	124.5
N(2)-H(2C)...Cl(5)#5	0.90	2.93	3.705(13)	145.4
C(1)-H(1E)...Cl(4)#4	0.96	2.82	3.759(19)	166.3
C(5)-H(5A)...Cl(1)#3	0.96	2.67	3.57(2)	156.3
293 K				

C(5)-H(5A)...Cl(1)#3	0.96	2.90	3.76(3)	149.4
N(2)-H(2C)...Cl(2)#4	0.90	2.44	3.13(2)	133.7
N(2)-H(2B)...Cl(1)	0.90	2.45	3.34(2)	168.2
N(2)-H(2A)...Cl(4)#1	0.90	2.43	3.213(16)	145.8
N(1)-H(1C)...Cl(4)#5	0.90	2.73	3.61(2)	167.1
N(1)-H(1B)...Cl(5)#5	0.90	2.87	3.38(2)	117.7
N(1)-H(1B)...Cl(2)#6	0.90	2.80	3.54(2)	140.5
N(1)-H(1A)...Cl(3)#7	0.90	2.91	3.33(2)	110.2
N(1)-H(1A)...Cl(3)#6	0.90	2.69	3.52(2)	154.5

Symmetry transformations used to generate equivalent atoms: **93K**, #1 -x+3/2,-y+1,z-1/2; #2 -x+3/2,-y+1,z+1/2; #3 -x+1,y-1/2,-z+1/2; #4 x-1/2,-y+1/2,-z; #5 -x+1,y-1/2,-z-1/2; #6 x-1/2,-y+3/2,-z; **223 K**, #1 -x,-y,z+1/2; #2 -x,-y,z-1/2; #3 x,y,z+1; #4 x+1/2,-y+1/2,z+1; #5 -x+1/2,y-1/2,z+1/2; #6 x+1/2,-y+1/2,z; #7 -x+1/2,y+1/2,z+1/2; **293 K**, #1 -x,-y,z+1/2; #2 -x,-y,z-1/2; #3 x,y,z+1; #4 -x+1/2,y-1/2,z+1/2; #5 x+1/2,-y+1/2,z; #6 x+1/2,-y+1/2,z+1; #7 -x+1/2,y+1/2,z+1/2.

Table S6 List of d_{33} measured value on different samples and comparison to reported value.

Piezoelectrics	*Measured direction*	*Measured* d_{33} (pC N^{-1})*	*Reference* d_{33} (pC N^{-1})	Source
$BaTiO_3$ (poling)	c-aixs**	105	85~95[1]	Purchased from Hefei Ke Jing Materials Technology Co., Ltd. http://www.kjmti.com/
$BaTiO_3$ (no poling)	c-aixs	10	> 0[2]	
DIPAB	b-aixs	11	11[3]	Prepared by ourselves according to the literature[4]
$LiNbO_3$	c-aixs	11	6~16[5]	Purchased from Hefei Ke Jing Materials Technology Co., Ltd. http://www.kjmti.com/
Rochelle salt	a-aixs	7	3~25[6]	Prepared by ourselves according to the literature[7]
KTP	b-aixs	6	6.1[8]	Purchased from Fujian CASTECH Crystals, Inc. http://www.castech.com/
Croconic acid	c-aixs	5	N/A	Prepared by ourselves according to the literature[9]
ZnO	c-aixs	3	2.3~3.5[10]	Purchased from Hefei Ke Jing Materials Technology Co., Ltd. http://www.kjmti.com/
Nylon-11	Thin film	2	2[11]	Purchased from ARKEMA, France http://www.arkema.com/en/
$[C_6N_2H_{18}][BiCl_5]$	**c-aixs**	**6**	**This work**	**This work**

* All measurement was done in our lab using d_{33} meter via Berlincourt method as described in Materials and Methods in Supplementary Materials. All measurement were carried out at room temperature, except for Rochelle salt which was studied at ~ 283 K.

** d_{33} of single crystalline BTO along [111] is reported to be $\geqslant$ 190 pC/N.[12,13]

References and Notes

[1] M. Zgonik, P. Bernasconi, M. Duelli, R. Schlesser, P. Günter, M. H. Garrett, D. Rytz, Y. Zhu, X. Wu, Dielectric, elastic, piezoelectric, electro-optic, and elasto-optic tensors of $BaTiO_3$ crystals. *Phys. Rev. B Condens. Matter* **50**, 5941–5949 (1994). doi:10.1103/PhysRevB.50.5941

[2] A. H. Meitzler, H. L. Stadler, Piezoelectric and dielectric characteristics of single-crystal barium titanate plates. *Bell Syst. Tech. J.* **37**, 719–738 (1958). doi:10.1002/j.1538-7305.1958.tb03884.x

[3] D. W. Fu, H.-L. Cai, Y. Liu, Q. Ye, W. Zhang, Y. Zhang, X.-Y. Chen, G. Giovannetti, M. Capone, J. Li, R.-G. Xiong, Diisopropylammonium bromide is a high-temperature molecular ferroelectric crystal. *Science* **339**, 425–428 (2013). doi:10.1126/science.1229675

[4] B. Xu, S. Ren, Integrated charge transfer in organic ferroelectrics for flexible multisensing materials. *Small* **12**, 4502–4507 (2016). doi:10.1002/smll.201600980

[5] R. S. Weis, T. K. Gaylord, Lithium-niobate: Summary of physical-properties and crystalstructure. *Appl. Phys., A Mater. Sci. Process.* **37**, 191–203 (1985). doi:10.1007/BF00614817

[6] E. Lemaire, R. Moser, C. J. Borsa, H. Shea, D. Briand, Green paper-based piezoelectric material for sensors and actuators. *Procedia Eng.* **120**, 360–363 (2015). doi:10.1016/j.proeng.2015.08.637

[7] A. S. Tayi, A. K. Shveyd, A. C.-H. Sue, J. M. Szarko, B. S. Rolczynski, D. Cao, T. J. Kennedy, A. A. Sarjeant, C. L. Stern, W. F. Paxton, W. Wu, S. K. Dey, A. C. Fahrenbach, J. R. Guest, H. Mohseni, L. X. Chen, K. L. Wang, J. F. Stoddart, S. I. Stupp, Room-temperature ferroelectricity in supramolecular networks of charge-transfer complexes. *Nature* **488**, 485–489 (2012). doi:10.1038/nature11395

[8] T. Jungk, A. Hoffmann, E. Soergel, Influence of the inhomogeneous field at the tip on quantitative piezoresponse force microscopy. *Appl. Phys., A Mater. Sci. Process.* **86**, 353–355 (2007). doi:10.1007/s00339-006-3768-9

[9] S. Horiuchi, Y. Tokunaga, G. Giovannetti, S. Picozzi, H. Itoh, R. Shimano, R. Kumai, Y. Tokura, Above-room-temperature ferroelectricity in a single-component molecular crystal. *Nature* **463**, 789–792 (2010). doi:10.1038/nature08731

[10] D. A. Scrymgeour, T. L. Sounart, N. C. Simmons, J. W. P. Hsu, Polarity and piezoelectric response of solution grown zinc oxide nanocrystals on silver. *J. Appl. Phys.* **101**, 014316 (2007). doi:10.1063/1.2405014

[11] E. K. Akdogan, M. Allahverdi, A. Safari, Piezoelectric composites for sensor and actuator applications. *IEEE Trans. Ultrason. Ferroelectr. Freq. Control* **52**, 746–775 (2005). doi:10.1109/TUFFC.2005.1503962

[12] R. Bechmann, Elastic, piezoelectric, and dielectric constants of polarized barium titanate ceramics and some applications of the piezoelectric equations. *J. Acoust. Soc. Am.* **28**, 347–350 (1956). doi:10.1121/1.1908324

[13] S. Wada, K. Yako, H. Kakemoto, T. Tsurumi, T. Kiguchi, Enhanced piezoelectric properties of barium titanate single crystals with different engineered-domain sizes. *J. Appl. Phys.* **98**, 014109 (2005). doi:10.1063/1.1957130